

# THE X-RAY SIGNATURE OF SOLAR CORONAL MASS EJECTIONS

R. A. HARRISON\*

*Department of Space Research, University of Birmingham, U.K.*

P. W. WAGGETT and R. D. BENTLEY

*Mullard Space Science Lab., University College London, U.K.*

K. J. H. PHILLIPS

*Rutherford Appleton Lab., Chilton, U.K.*

M. BRUNER

*Lockheed Palo Alto Research Labs., Calif., U.S.A.*

M. DRYER

*Space Environment Lab., NOAA-ERL, Boulder, Colo., U.S.A.*

and

G. M. SIMNETT

*Department of Space Research, University of Birmingham, U.K.*

(Received 28 May, 1984; in final form 19 April, 1985)

**Abstract.** The coronal response to six solar X-ray flares has been investigated. At a time coincident with the projected onset of the white-light coronal mass ejection associated with each flare, there is a small, discrete soft X-ray enhancement. These enhancements (precursors) precede by typically  $\sim 20$  m the impulsive phase of the solar flare which is dominant by the time the coronal mass ejection has reached an altitude above  $0.5 R_{\odot}$ . We identify motions of hot X-ray emitting plasma, during the precursors, which may well be a signature of the mass ejection onsets. Further investigations have also revealed a second class of X-ray coronal transient, during the main phase of the flare. These appear to be associated with magnetic reconnection above post-flare loop systems.

## 1. Introduction

Mass ejection must be regarded as a primary constituent of the solar flare process since it accounts for a large fraction of the total flare energy (Rust *et al.*, 1980). A flare model which does not describe such ejection is ignoring a cornerstone of the flare phenomenon. However, it has become apparent that coronal disturbances frequently, if not always,

\* Present address: High Altitude Observatory, National Center for Atmospheric Research, Boulder, Colo., U.S.A. NCAR is sponsored by the National Science Foundation.

commence some time prior to the main flare onset (Jackson and Hildner, 1978; Jackson, 1981; Wagner, 1983) and, as we shall demonstrate, can be associated with soft X-ray precursor activity (see also Simnett and Harrison, 1985). These features place stringent limits on any flare model. Furthermore, a model is required to explain why some ejecta are flare-related and some not. The relative timing and importance of some flare-related events and low coronal behaviour of the transient are not well known; some clarification is necessary.

The notion of 'time-zero', that is the time of the first energy release, has been addressed in the review by Dryer (1982) who noted that with respect to coronal mass ejections most attention in the past has been directed to the moment when microwave radio bursts and suprathermal electron jets (with associated type III emission) occur more or less simultaneously with the onset of H $\alpha$  emission. He noted that 'it should not come as any surprise that pre-flare (coronal) activity should be detected...'. We will demonstrate the initiation of several coronal transients at low levels in the corona as a result of flare-precursor activity in soft X-rays observed by the Hard X-ray Imaging Spectrometer on the Solar Maximum Mission satellite.

From an extensive study of solar X-ray images, primarily taken during the limb crossing of a particular group of active regions, we are led to identify X-ray counterparts to white-light Coronal Mass Ejections (CMEs), which we shall call X-ray coronal transients. These fall into two categories. One class is clearly associated with white-light CMEs and soft X-ray precursors, whereas the other class has no known white-light component and is not associated with any detectable fresh energy release.

The June 29, 1980 period will be used to illustrate the majority of our investigations. A discussion on the onset phase of CMEs is presented in Section 3, followed by a look at the relevance of our findings to an MHD model of the corona in Section 4.

## 2. Observations

### 2.1. THE ACTIVITY OF JUNE 29, 1980

On June 29, 1980, five active regions were positioned on the western solar limb between the southern latitudes of 20 to 35 degrees (Harrison *et al.*, 1984). Four large flares are registered from 02:33 UT, 10:41 UT, 18:03 UT, and 18:23 UT, having GOES soft X-ray importance M3, M4, M1, and M4, respectively. White-light CMEs associated with three of these flares were recorded by the Coronagraph/Polarimeter (C/P, MacQueen *et al.*, 1980), onboard the Solar Maximum Mission (SMM), and the ground-based High Altitude Observatory's K-Coronameter at Mauna Loa.

The onsets of the coronal mass ejecta are found to be in close association with 3.5–5.5 keV X-ray precursor events seen by the Hard X-Ray Imaging Spectrometer (HXIS, van Beek *et al.*, 1980), also on SMM, before the 02:33 UT and 10:41 UT flares, and with the 18:03 UT flare, which can be thought of as a bright precursor to the larger 18:23 UT event. This association has stimulated the model due to Simnett and Harrison (1985) where the 'main' flare is considered to be a 'knock-on' event

following the precursor event and CME onset. Further investigations are shown here to reveal X-ray motions, at the onset time of the CMEs, which may well be part of the rising structure. Moreover, late into the flares we find evidence for a second class of X-ray coronal transient which may relate to the magnetic reconnection of post-flare loops (Kopp and Pneuman, 1976).

The above observations are supported by additional data collected on March 30, April 7 and June 26 of 1980.

## 2.2. THE JUNE 29, 02:33 UT FLARE

The 3.5 – 5.5 keV X-ray intensity-time profile for the June 29, 02:33 UT flare is reproduced in Figure 1 with the projected altitude history of the associated white-light

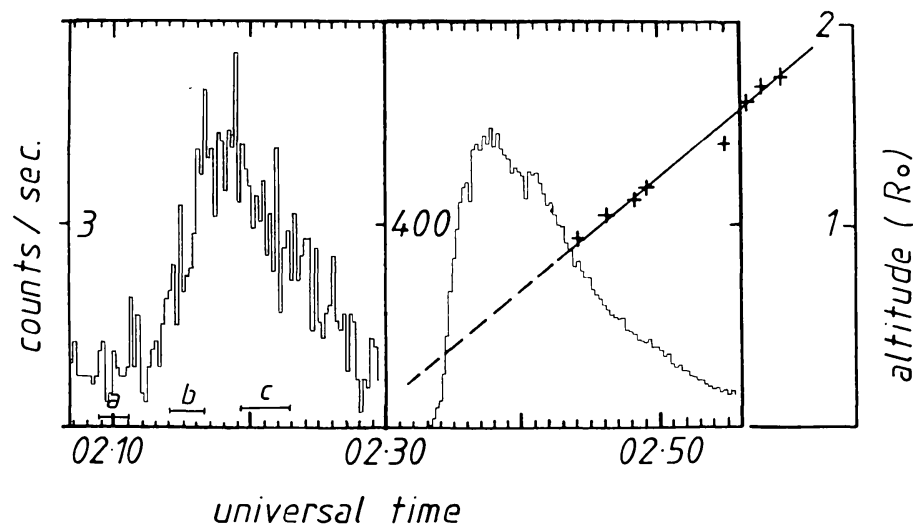


Fig. 1. The relationship between the June 29, 1980, 02:33 UT flare and the first June 29 white-light coronal mass ejection. The 3.5 to 5.5 keV intensity-time profile is shown for the flare (post-02:30 UT) and its precursor (pre-02:30 UT). Note the scale change at 02:30 UT. Superimposed onto this are the altitude histories of the white-light coronal mass ejection and an X-ray transient which is shown in Figure 2. The solid line is a best fit to the observed leading edge locations of the ejection, shown as crosses (Gary, 1982), and the dashed line is a projection with assumes no acceleration.

CME superimposed onto it. The M3 flare is recorded from 02:33 UT but there is clearly a weaker, precursor event which peaks at about 02:18 UT at  $\sim 8$  times the background intensity level. At maximum, the precursor emission displays a temperature of  $(1.1 \pm 0.2) \times 10^7$  K with an emission measure of approximately  $3 \times 10^{46} \text{ cm}^{-3}$ . These figures are obtained from the Counting Rate Prediction Program (Mewe, 1983; based on work by Gronenschild and Mewe, 1978). Assuming no acceleration and a low-level onset, the CME started at 02:28 UT some five minutes prior to the main flare onset (Gary, 1982); the onset of the hard X-ray burst is at 02:33 UT. Figure 1 implies a correlation between the X-ray precursor and the mass ejection onset, which is strengthened if some acceleration is assumed. At 02:33 UT the CME altitude is  $2.1 \times 10^5$  km which we consider to be too high for the onset location. Alternatively, the

data-points of Figure 1 could be consistent with a low-level CME onset at flare onset if the CME undergoes deceleration. Few, if any, decelerating mass ejections have been observed (Wagner, 1983).

A search in the HXIS 3.5–5.5 keV image data has resulted in the identification of plasma motion, or at least brightness motion, at the time of the CME onset. Figure 2

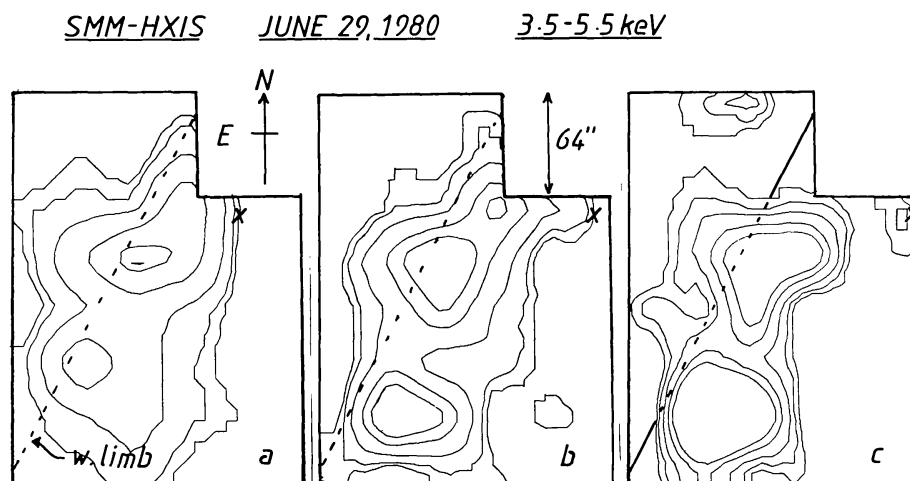


Fig. 2. The X-ray transient seen in the precursor phase of the first June 29 flare. Three HXIS 3.5 to 5.5 keV images are shown for accumulations at (a) 02:08:41 UT for 84.5 s, (b) 02:13:49 UT for 84.5 s, and (c) 02:18:56 UT for 122.9 s. Intensity contours are plotted at 0.28, 0.21, 0.14, 0.07, 0.04, and 0.023 counts  $s^{-1}$ . The altitudes of the three crosses are plotted in Figure 1 (labelled *a*, *b*, and *c*). Note the 50% duty cycle; the 84.5 s accumulations are made over 169 s. For all HXIS images shown in this paper the background level is  $\sim 0.005$  counts  $s^{-1}$  per pixel, the solar west limb is shown with the Sun to the left and the data are corrected for the collimator response of the instrument.

shows three HXIS 32'' resolution images taken during the precursor, the first of which delineates a hot coronal loop feature, the southern leg of which is to be the site of the flare. To the south of this loop is a second bright patch. As the precursor progresses, the southern side of the loop and the second bright patch become considerably enhanced. Note that in Figure 2 the intensity contour levels are uniform between images. The locations of the two brightest patches, as identified by Harrison *et al.* (1984), remain fixed from image to image and there are various transient features. The small patch which becomes visible to the north of the last image is identified by Harrison *et al.* (1984) as being in the vicinity of another active region. The one feature that displays continual, weak outward motion is seen in the extreme north-west corner of the Figure 2 images. The  $2.3 \times 10^{-2}$  counts  $s^{-1}$  contour level ( $5 \times$  background) at the front of this outward moving feature is marked with a cross and the altitudes of the crosses are plotted in Figure 1. The motion is consistent with a velocity of  $\sim 55$  km  $s^{-1}$  ( $0.3 R_{\odot} \text{ hr}^{-1}$ ) and an examination of the altitude profiles in Figure 1 shows that this feature may well be an early signature of part of the ascending structure characterized later by the white-light CME, assuming some acceleration. However, we need to use extreme care in relating

X-ray and coronagraph data since we cannot be sure of the relative degree to which mass motions are indicated in the two sets of data.

This weak, ascending feature was also detected by the X-ray Polychromator (XRP, Acton *et al.*, 1980) onboard SMM. The four HXIS pixels in the northwest corner of the image, through which the X-ray transient passes, show a declining 5.5–8.0 keV to 3.5–5.5 keV intensity ratio despite a >4-fold intensity enhancement in the lower channel, between images *a* and *c* of Figure 2. This increase in emission measure suggests, then, that we are seeing a density enhancement as the transient passes. We believe this to be due to the outward motion of material, although an alternative explanation would be for successively higher loops to be heated.

There is much less mass involved in the precursor emission than in the white-light CME. At an emission measure ( $N_e^2 V$ ) of  $3 \times 10^{46} \text{ cm}^{-3}$  and assuming an electron density ( $N_e$ ) of  $10^9 \text{ cm}^{-3}$ , the precursor involves a mass of ( $N_e V m_H$ )  $\sim 5 \times 10^{13} \text{ g}$  which is an order of magnitude less than that estimated by Gary (1982) for the mass of the loop transient. Furthermore, as Figure 2 indicates, only a small fraction of the precursor emission is involved with the ejection. The precursor, in total, involves structures of the scale of the active region itself.

There is a metric type II radio burst associated with this event. Wagner (1983) and Gary (1982) believe that the extrapolated onset time for the type II related disturbance is at flare onset which, we believe, is not the CME onset time. This is consistent with the type II being a signature of a flare driven shock and not a precursor driven shock.

No other fresh white-light coronal manifestation of the 02:33 UT flare is reported, yet there is evidence for a second X-ray coronal transient from 02:40 UT, which is stronger than the precursor related X-ray transient. Figure 3 shows a series of 3.5–5.5 keV intensity images taken during the decay phase of the main flare. This transient is seen crossing the northwest corner of the HXIS image from the loop-top, at speeds as low as  $20 \text{ km s}^{-1}$ . Assuming no decay, this X-ray transient would reach the C/P field of view several hours after the flare and thus may be difficult to identify.

The 64" square, occupying the northwest corner of the HXIS field of view of Figure 3, images a purely coronal region through which the X-ray transient passes. The 3.5–5.5 keV and 5.5–8.0 keV intensity profiles for this square indicate a steady increase in emission measure from about  $9.2 \times 10^{46} \text{ cm}^{-3}$  to  $2.9 \times 10^{49} \text{ cm}^{-3}$  between 02:44 UT. We regard this increase as a signature of a density increase due to plasma motion. From 02:44 UT the emission measure is seen to drop slowly. The timing, location, direction of motion and lack of association with a fresh energy release are consistent with this second X-ray transient being the signature of a rising neutral point above post-flare reconnecting loops. Note that this motion is seen in association with an event which has been shown to have longlived overlying loop structures (Harrison *et al.*, 1984). These structures are of the type discussed by Švestka *et al.* (1982).

Despite a thorough data-search, we have been unable to identify any other X-ray coronal transients at any stage in this event. This search was done by comparing the flare-onset structure to subsequent activity until spacecraft night, and by comparing successive accumulations throughout the event.

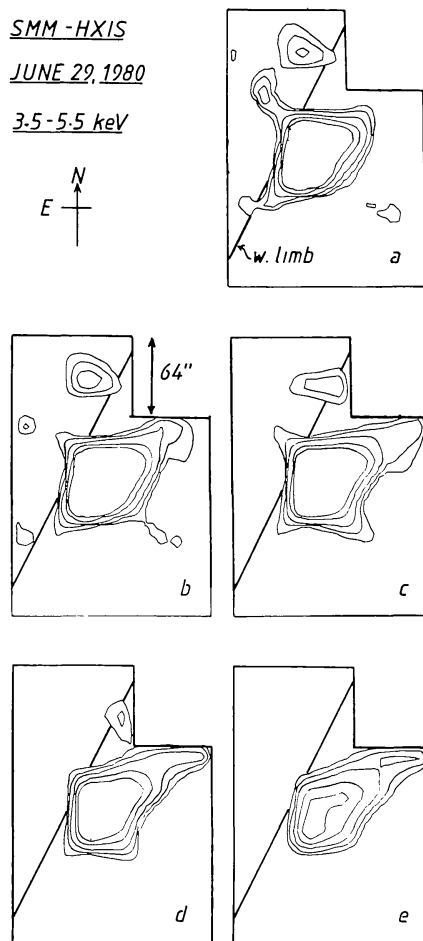


Fig. 3. The X-ray transient seen during the first June 29 flare. A series of HXIS 3.5 to 5.5 keV images are shown for accumulations at (a) 02:36:58 UT for 9.2 s, (b) 02:39:50 UT for 9.2 s, (c) 02:43:45 UT for 12.3 s, (d) 02:49:54 UT for 24.6 s, and (e) 02:54:57 UT for 61.4 s. Intensity contours are plotted at 50, 25, 10, 5, and 2.5 counts  $s^{-1}$ .

### 2.3. THE JUNE 29, 10:41 UT FLARE

The X-ray component of the flare of June 29, 10:41 UT is similar to that of the 02:33 UT event. It occupies the same magnetic flux loop (compare the images of Figures 3 and 6) and has a similar intensity-time profile. The C/P suffered a black-out from 10:48 UT to 13:20 UT but Wagner (1983) and Hundhausen (1984) believe that post-flare data are indicative of the recent passage of a CME. Figure 4 shows the 3.5–5.5 keV intensity-time profile of this flare. From 10:28 UT, some 13 min prior to the main flare onset, a finger of UV-emitting plasma (Oxygen V line at 1371 Å) is seen to project into the corona from the southern footpoint of the large loop of Figure 2, so there is evidence for a coronal event associated with the X-ray precursor. In this same location, from about 10:23 UT, HXIS detected an X-ray transient as shown in Figure 5. Again, the leading edge of the transient is marked with a cross and its altitude

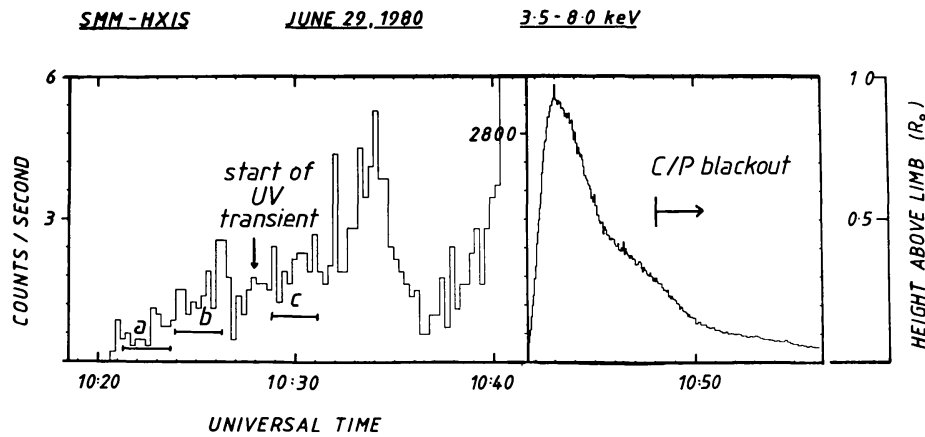


Fig. 4. The relationship between the June 29, 1980 10:41 UT flare and associated coronal activity. The 3.5 to 5.5 keV intensity-time profile is shown for the flare (post-10:42 UT) and its precursor (pre-10:42 UT). Superimposed onto this is the altitude history of an X-ray transient which is shown in Figure 5. Also shown is the C/P blackout period and the onset time of a UV coronal transient.

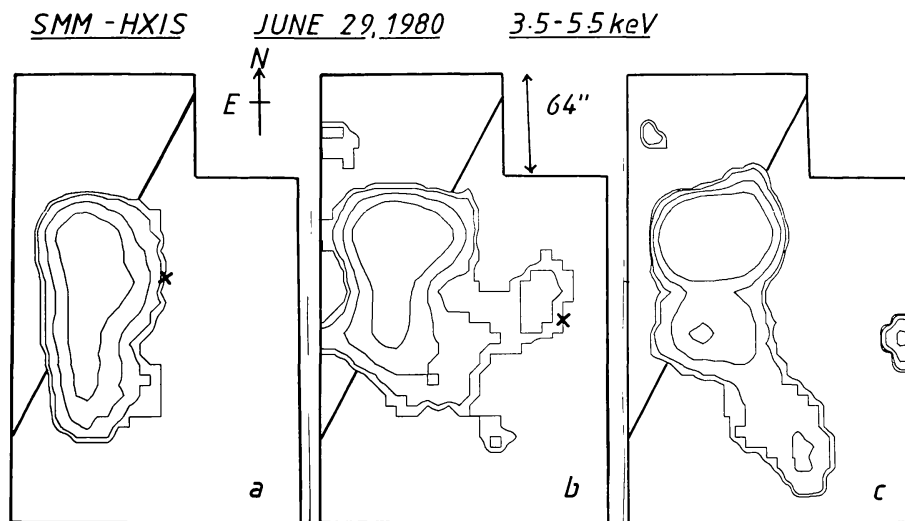


Fig. 5. The X-ray transient seen in the precursor phase of the second June 29 flare. Three HXIS 3.5 to 5.5 keV images are shown for accumulations at (a) 10:21:00 UT for 76.8 s, (b) 10:23:36 UT for 76.8 s, and (c) 10:28:41 UT for 76.8 s. Intensity contours are plotted at 0.2, 0.1, 0.06, 0.03, and 0.015 counts  $s^{-1}$ . The altitudes of the crosses, plus a projected altitude for the patch crossing the edge of the third image, are plotted in Figure 4.

is plotted in Figure 4. We conclude that the scenario is similar to the 02:33 UT flare transient, despite the lack of C/P data, namely that a mass ejection is initiated during the precursor. The finger of emission in Figure 5, extending into the corona to the southeast of the transient, is one of the stable loops identified by Harrison *et al.* (1984) (see their Figures 8 and 9).

A thorough data-search revealed a further example of a slow X-ray transient as illustrated in Figure 6. From 10:43 UT a tongue of plasma originating from the loop-top

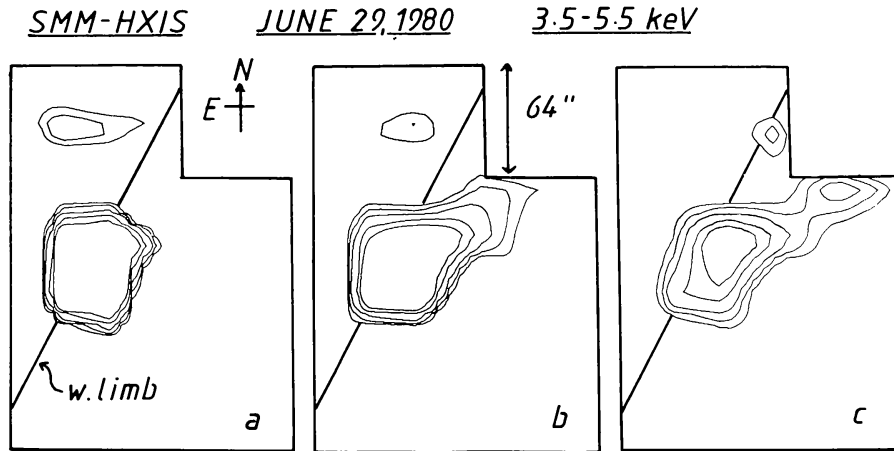


Fig. 6. The X-ray transient seen during the second June 29 flare. Three HXIS 3.5 to 5.5 keV images are shown for accumulations at (a) 10:46:00 UT for 13.9 s, and (c) 10:53:34 UT for 20.5 s. Intensity contours are plotted at 100, 50, 20, 10, and 5 counts  $s^{-1}$ .

is observed to cross the corona at about  $60 \text{ km s}^{-1}$ . The ejection is very similar to that of 02:40 UT and also occurs in the main phase of the flare. Again, an emission measure increase along with no temperature rise is observed in the coronal pixels as the event progresses implying the passage of a mass transient which we associate with post-flare reconnection.

#### 2.4. THE JUNE 29, 18:00 UT FLARES

Figure 7 shows the intensity-time profiles for the June 29, 18:03 UT and 18:23 UT

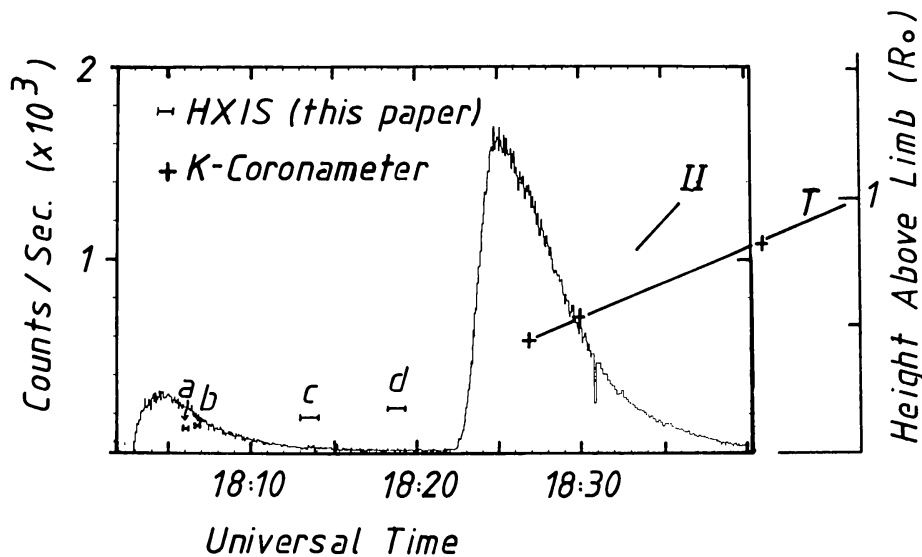


Fig. 7. The relationship between the June 29, 18:00–19:00 UT flares and associated coronal activity. The 3.5 to 5.5 keV intensity time profile is shown for the 18:23 UT flare and the smaller 18:03 UT event. Superimposed onto this are the altitude histories of a three-minute type II radio burst (labelled II), a white-light coronal mass ejection (labelled T) and an X-ray transient shown in Figure 8.



flares. Superimposed onto the curves are the altitude histories of the white-light transient ( $T$ ), the associated type II disturbance (II) (both from Wu *et al.*, 1983) and the estimated altitudes of an X-ray transient. The white-light CME is associated with a small event preceding a larger flare, and again, the association is stronger if acceleration is considered; the onset time assuming no acceleration is projected to be 18:11 UT. However, an examination of the High Altitude Observatory's  $K$ -coronameter data, in fact, clearly shows the white-light CME propagating through the corona prior to flare onset (Sime, 1985). At 18:18 UT, some five minutes prior to the flare onset, the peak density of the CME is at  $\sim 0.34 R_{\odot}$  and at 18:21 UT it is at  $\sim 0.4 R_{\odot}$ . Thus the CME clearly had a pre-flare onset. We regard the 18:03 UT flare as a large precursor to the 18:23 UT flare. In this event the type II and CME events appear to represent different disturbances, the type II projecting back to the limb region at the 'main' flare onset. Figure 8 shows evidence for an X-ray transient from  $\sim 18:06$  UT with a velocity of

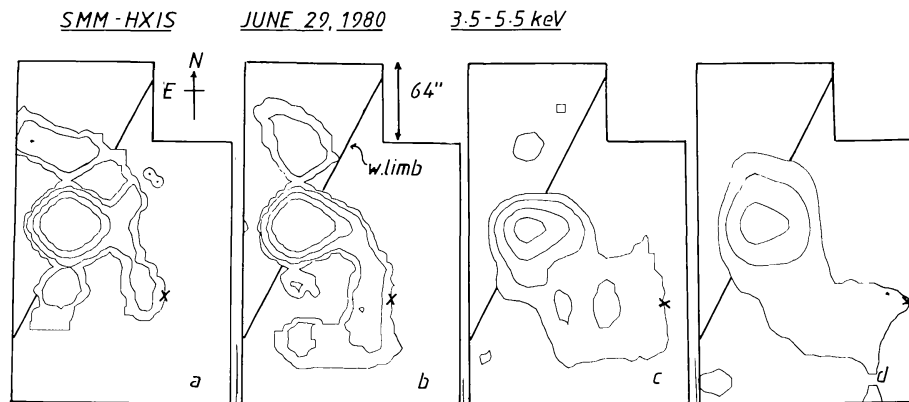


Fig. 8. The X-ray transient seen in the precursor phase of the last June 29, 1980 flare. A series of HXIS 3.5 to 5.5 keV images are shown for accumulations at (a) 18:05:48 UT for 7.7 s, (b) 18:06:16 UT for 7.7 s, (c) 18:18:07 UT for 32.2 s. Intensity contours are plotted at 20, 5, 1, and 0.2 counts  $s^{-1}$ . The altitudes of the crosses which denote the leading edge of the transient are plotted in Figure 7.

$< 40 \text{ km s}^{-1}$ . The white-light CME velocity is recorded at  $300 \text{ km s}^{-1}$  some 20 min later. These may be signatures of the same ascending structure which underwent a period of acceleration. The altitudes of the crosses marked on Figure 8, at the leading edge of the X-ray transient, are plotted in Figure 7 and labelled  $a$  to  $d$ . The first two images of Figure 8 appear to show a brightening of one of the loops proposed by Harrison *et al.* (1984). This loop is clearly visible in the second image. However, the later two images show brightness contours extending outwards from the region of the loop-top. Pixels to the extreme west of the images indicate a density enhancement along with the passage of the transient.

As with the 02:33 UT and 10:41 UT flares, motion is detected in the corona during the main phase of the 18:23 UT event. Evidence for this is shown in Figure 9, the transient again crossing the northwest corner of the images, at a velocity of

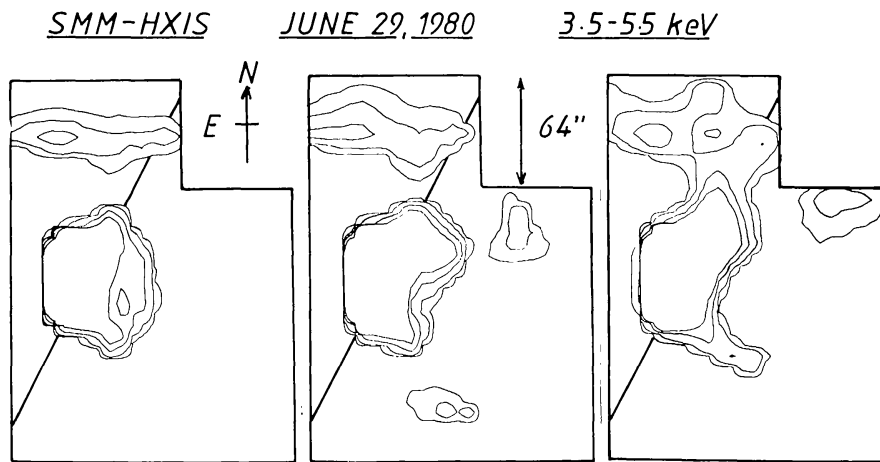


Fig. 9. The X-ray transient seen during the last June 29 flare. Three HXIS 3.5 to 5.5 keV images are shown for accumulations at (a) 18 : 24 : 00 UT for 4.6 s, (b) 18 : 25 : 01 UT for 4.6 s, and (c) 18 : 28 : 55 UT for 7.7 s. Intensity contours are plotted at 20, 10, 3, and 1.5 counts  $s^{-1}$ .

$\sim 30 \text{ km s}^{-1}$ . During this event a second active region, to the north of the flare, becomes considerably enhanced and there is evidence for activity within the loop feature extending to the south (Harrison *et al.*, 1984), which was seen in Figures 5 and 8.

## 2.5. OTHER EVENTS

In this study we examine activity tens of minutes prior to a flare as well as during the flare itself. This means that out of the several hundred flares observed by the imaging instruments on SMM, which had an observing window of  $\sim 60$  min per orbit, few will be sufficiently well viewed. In addition, since we want to link surface observations to C/P data, we are limited to near-limb events. The June 29 flares were particularly well observed. We describe below three more events in 1980 which are found to fit the same pattern.

Prior to the long duration X-ray flare of 13 : 10 UT on 1980, March 30 (Lantos *et al.*, 1981), a weak, soft X-ray precursor was observed by SMM between 12 : 47 UT and 12 : 50 UT (Waggett *et al.*, 1985). Lantos and Kerdraon (1984) demonstrate that the motion of a metric noise storm and a subsequent CME are consistent with the rising of a loop feature at a constant velocity of  $370 \text{ km s}^{-1}$  from 13 : 00 UT when the loop-top was at  $10^5 \text{ km}$ . Projecting this to the chromosphere would suggest a  $\sim 15$  min pre-flare onset for the CME, and, allowing for some initial acceleration, would imply a CME-onset/X-ray precursor association as with the June flares (see Waggett *et al.*, 1985).

On April 7 a CME was observed by C/P at  $28^\circ$  west of north, crossing the solar corona at  $700 \text{ km s}^{-1}$ . The position indicated an association with Active Region 2372 at N 14 W 05. The projected onset time, assuming no acceleration, was 03 : 20 UT, just after a weak, soft X-ray burst observed by HXIS in AR 2372. Unfortunately, SMM went into the Earth's shadow at 03 : 27 UT but a -N flare was reported at 03 : 34 UT

from AR 2372. Once again, we are seeing a 'main' flare preceded by a small X-ray burst which is associated with the CME onset.

Our final example is from June 26 when a C4 flare was observed by HXIS from 19:45 UT in AR 2522 at S 30 W 41. C/P detected a CME originating from the vicinity of the flare, whose projected onset time was 19:15 UT (Illing, 1984), during SMM night. However, the C4 flare is associated with a -B H $\alpha$  flare and from the same region, at 19:15 UT, there was a -F H $\alpha$  event observed as a small burst in the 1–8 Å GOES X-ray record. We believe this to be a signature of the precursor activity; we also believe that it is associated with the CME onset. Apart from these two events, there is no H $\alpha$  activity between 17:26 UT and 21:49 UT (*Solar Geophysical Data*, U.S. Dept. of Commerce).

### 3. The Coronal Mass Ejection Onset

The six solar X-ray events studied demonstrate that there is a close association between X-ray flare precursor activity and the initial ejection of material, and that the association is stronger if we assume an early acceleration phase in the CME. One may also consider two other possibilities. Firstly, the CME may be launched at the flare onset time from a low altitude, initially experiences rapid acceleration and then rapidly decelerates to a somewhat constant velocity. Secondly, the CME may be launched at a high altitude at the time of flare onset and rise with a relatively constant velocity.

Let us examine these two possibilities within the context of the six events discussed above. The rapid acceleration followed by rapid deceleration seems rather unlikely and is not considered further. Assuming a constant CME velocity, the average CME altitude at flare-onset is  $\sim 0.66 R_{\odot}$  above the active region. This is within the C/P and K-coronameter fields of view. Initiation of the CME by a fast moving disturbance, at some altitude, during the flare onset, seems improbable. For example, for an Alfvén wave (velocity =  $B/\sqrt{4\pi mN}$ ) to travel  $0.66 R_{\odot}$  through a medium of density ( $N$ )  $10^{10} \text{ cm}^{-3}$  and field strength ( $B$ ) 10 G, we expect a crossing time of  $\sim 40$  min. A disturbance travelling at the ion-sound speed at  $T \sim 10^7$  K would cross the same distance in  $\sim 25$  min.

### 4. A Coronal MHD Model: Revisited

As mentioned in the introduction, the MHD modellers were aware of the potential influence of the precursor events. In all of their applications, however, they chose to confine themselves to the main events. As a result of the present observations, we now re-examine the model results of Wu *et al.* (1983) for the 18:23 UT flare of June 29. In that paper, the XRP results for the density and temperature, starting at about 18:22 UT, were used to infer a temporal, triangular pressure pulse. Consequently, the trajectory of the peak density in the model CME moved outward with the same velocity as that for the K-coronameter transient. However, it was displaced some  $0.25 R_{\odot}$  below the actual CME. A high amplitude MHD wave preceded the peak density in the model

transient, but a shock did not form. In the event, a shock did form, albeit for only three minutes, ahead of the peak density in the actual CME (Figure 7). We will now re-examine these events with the following general discussion.

With the benefit of hindsight afforded by the present X-ray results, we suggest that the sequence of events may be clarified as follows for the 18:23 UT flare and the 18:03 UT precursor event. First, we estimated the temporal pressure increase for the latter event; it was found that the temperature increased to  $2 \times 10^7$  K at 18:04 UT followed by a rapid decay to about  $0.7 \times 10^7$  K at 18:08 UT. During this same interval, the density increased to  $10^{11}$  cm<sup>-3</sup> and decayed to background ( $10^8$  cm<sup>-3</sup>). Thus, the peak pressure pulse was about one quarter that of the 'main' flare at 18:23 UT. As shown in the early MHD modelling work, transient atmospheric response is found for a wide spectrum of temporal durations that range from impulsive energy releases to longer lasting piston-driven pulses (see e.g. Dryer, 1982, and references therein). Thus the corona above the briefly enhanced loops of the precursor will respond by a combined wave and mass motion; i.e. a CME that would move with a relatively low velocity as a result of the modest energy release.

Examination of Figure 8 shows that, indeed, a low-velocity X-ray transient motion was detected. An estimate of the heights above the limb at these times places their peak density points earlier and slightly above an extrapolated line from the *K*-coronameter observation of Wu *et al.* (1983). Acceleration is definitely indicated by a linkage of the HXIS and *K*-coronameter data. Also, as suggested earlier, this acceleration would, to build upon the MHD model analogy, produce fast mode waves that would have evolved from simple waves early in the event to steepening non-linear waves (especially after the steep rise at 18:23 UT) and, finally, into a shock wave at the time of the type II emission. This assumes that the type II and the CME are signatures of the same rising structure. The shock then ran ahead of the CME at a higher velocity before it decayed back into a non-linear MHD wave. We can only speculate that the shock's decay was the result of a coronal spatial change wherein the local Alfvén speed increased; that is, the shock Mach number briefly exceeded 1.0 for only a three-minute period. We plan to make an explicit re-calculation of the MHD model by using the triangular pressure pulse described above for the precursor. In a future report, we hope to (a) show that the above suggestions for the precursor-initiated CME constitute a reasonable explanation for part of the chain of cause-and-effect, and (b) identify more precisely the relationship between the CME and type II disturbances.

## 5. Summary

In summary, we make the following statements:

- (1) Data from six solar X-ray events indicate that a CME-onset occurs in conjunction with a weak burst identified in soft X-rays and H $\alpha$ . In these events a 'main' flare follows some tens of minutes later, prompting us to label the weak burst as a precursor.
- (2) We find evidence for a class of X-ray coronal transient; this evidence may be a

signature of part of the initial rising of the CME structure. This being the case, the data support CME acceleration.

(3) We also find evidence for a second class of X-ray coronal transient. These events are not associated with fresh energy release or new surface activity. They are thought to be the signature of rising plasma carried in the magnetic fields above ascending neutral points in magnetically reconnecting post-flare systems.

(4) For two events on June 29, we suggest that the disturbance responsible for the CME may be different from that responsible for the type II emission (see Wagner and MacQueen, 1983). Certainly since we assign the CME to a precursor-related disturbance we need to ask whether the type II is precursor or flare related. Time-altitude profiles imply the latter. The CMEs do, however, display acceleration which would lead to a steepening of fast mode MHD waves, possibly eventually producing a shock.

What do the above observations mean to the flare process? If the precursor and CME lead the main flare in the way described, then a flare model must account for the pre-flare stages; the 'main' flare-burst is a secondary event. Simnett and Harrison (1985) present a model whereby particle acceleration results in the heating of the contents of a coronal loop. If some particles are given sufficient energy to descend to the transition region at one of the footpoints then we may see an X-ray signature; this is the precursor. If the thermal pressure in the loop increases sufficiently to destabilize the loop, the plasma is effectively free and may propagate through the corona as a CME. Acceleration at the CME front combined with energetic particle feedback along the field lines may produce the flare. If the field lines are disrupted we may not observe a flare event. This model clearly allows for a spectrum of events. As the field lines close down, after the passage of the CME, the post-flare loops are observed as described above.

Relatively few observational sequences have been performed where near-limb X-ray and UV images have been made along with corroborative coronagraph and radio investigations. Such an effort is essential for pinning down the relationship between X-ray activity and coronal events.

### Acknowledgements

The development and construction of the Hard X-ray Imaging Spectrometer was made possible by support given by the Netherlands Ministry for Education and Science through the Committee for Geophysics and Space Research of the Royal Netherlands Academy of Arts and Sciences, and the Science and Engineering Research Council (SERC) of the United Kingdom.

We gratefully acknowledge the many discussions and collaborations initiated by the Solar Maximum Mission Workshop series held at the Goddard Space Flight Center, Maryland, organized jointly by the National Aeronautics and Space Administration and the University of Maryland, and the U.K. – Solar Maximum Mission Workshop series held at Oxford, England, organized jointly by SERC and the U.S. Office of Naval Research. We are particularly grateful to Drs E. Hildner, B. V. Jackson, R. M. MacQueen, and A. J. Hundhausen for helpful ideas and comments.

R. A. H. and P. W. would like to express their gratitude to the SERC for financial support. M. D. was supported via NASA Interagency Agreement No. W153-61 and USAF AFGL Project Order RESD-84-619.

### References

- Acton, L. W., Culhane, J. L., Gabriel, A. H., and 21 co-authors: 1980, *Solar Phys.* **65**, 53.  
 Dryer, M.: 1982, *Space Sci. Rev.* **33**, 233.  
 Gary, D. E.: 1982, Ph. D. thesis, University of Colorado.  
 Gronenschild, E. H. B. M. and Mewe, R.: 1978, *Astron. Astrophys. Suppl.* **32**, 283.  
 Harrison, R. A., Simnett, G. M., Hoyng, P., Lafleur, H., and van Beek, H. F.: 1984, *Proc. STIP Symp. on Solar/Interplanetary Intervals*, p. 287.  
 Hundhausen, A. J.: 1984, private communication.  
 Illing, R. M. E.: 1984, private communication.  
 Jackson, B. V.: 1981, *Solar Phys.* **73**, 133.  
 Jackson, B. V. and Hildner, E.: 1978, *Solar Phys.* **60**, 155.  
 Kopp, R. A. and Pneuman, G. W.: 1976, *Solar Phys.* **50**, 85.  
 Lantos, P., Kerdraon, A., Rapley, C. G., and Bentley, R. D.: 1981, *Astron. Astrophys.* **101**, 33.  
 Lantos, P. and Kerdraon, A.: 1984, submitted to *Solar Phys.*  
 MacQueen, R. M., Csoeke-Poeckh, A., Hildner, E., House, L. L., Reynolds, R., Stanger, A., Tepoel, H., and Wagner, W. J.: 1980, *Solar Phys.* **65**, 91.  
 Mewe, R.: 1983, private communication.  
 Rust, D. M. and Hildner, E.: 1976, *Solar Phys.* **48**, 381.  
 Rust, D. M. *et al.* 1980, in Sturrock, P. A. (ed.), *Solar Flares*, Colorado Associated University Press, p. 273.  
 Sawyer, C., Simnett, G. M., Erskine, F. T., and Gergely, T.: 1984, *Proc. STIP Symp. on Solar/Interplanetary Intervals*, p. 237.  
 Sime, D. G.: 1985, private communication.  
 Simnett, G. M. and Harrison, R. A.: 1985, *Solar Phys.*, submitted.  
 Švestka, Z., Stewart, R. T., Hoyng, P., and 12 co-authors: 1982, *Solar Phys.* **75**, 305.  
 van Beek, H. F., Hoyng, P., Lafleur, H., and Simnett, G. M.: 1980, *Solar Phys.* **65**, 39.  
 Waggett, P. W., Simnett, G. M., Bentley, R. D., Harrison, R. A., and Lantos, P.: 1985, in preparation.  
 Wagner, W. J.: 1983, *Adv. Space Res.* **2**, 203.  
 Wagner, W. J. and MacQueen, R. M.: 1983, *Astron. Astrophys.* **120**, 136.  
 Wu, S. T., Wang, S., Dryer, M., Poland, A. I., Sime, D. G., Wolfson, C. J., Orwig, G. E., and Maxwell, A.: 1983, *Solar Phys.* **85**, 351.